Received: 15 December 2023 | Revised: 23 February 2024 | Accepted: 8 March 2024

DOI: 10.1002/pc.28328

RESEARCH ARTICLE

Polymer COMPOSITES WILEY

Enhancing damage resistance in tubular triaxial hybrid braided composites: Innovative production and tensile modulus prediction with damage analysis

Ghazal Ghamkhar[1,2] | **Majid Safar Johari**[2] | **Mahdi Bodaghi**[1]

[1]Department of Engineering, School of Science and Technology, Nottingham Trent University, Nottingham, UK

[2]Department of Textile Engineering, Amirkabir University of Technology, Valiasr Square, Tehran, Iran

Correspondence
Mahdi Bodaghi, Department of Engineering, School of Science and Technology, Nottingham Trent University, Nottingham NG11 8NS, UK.
Email: mahdi.bodaghi@ntu.ac.uk

Abstract

Braided composite structures, characterized by their inherent brittleness, necessitate precise damage prediction and prevention to ensure structural integrity/reliability. This study introduces an innovative method for enhancing damage resistance in tubular triaxial hybrid braided composites. These composites employ Epoxy resin as the matrix, with polyester serving as the bias yarn, and glass and basalt as the axial yarns, woven at varying braiding angles. Tensile tests reveal a compelling trend: a reduction in the braiding angle correlates with an increase in the failure load, indicative of quasi-ductile behavior. A model is also derived for predicting tensile elastic modulus, which demonstrates a strong correlation with experimental results. Furthermore, finite element simulations are utilized to analyze damage within the triaxial hybrid braided composite specimens, providing empirical confirmation of progressive damage occurrence. This research offers a promising avenue for designing/manufacturing advanced composite materials with superior damage-resistance holding immense potential across a spectrum of engineering applications.

Highlights

- The tubular triaxial hybrid braided composites were produced by Epoxy resin as the matrix, with polyester as the bias yarn, and glass and basalt as the axial yarns at different braiding angles.
- An innovative method was introduced for enhancing damage resistance in tubular triaxial hybrid braided composites.
- The effect of operating parameters (braiding angle, type of bias yarns, production method) was investigated.
- Was tried to predict tensile modulus values in tubular triaxial hybrid braided composites by finite element simulation and developed equations.
- Finite element simulation exhibited excellent performance in the prediction of tensile behavior of structures manufactured by the innovative method.

KEYWORDS
damage, hybrid braided composite, tensile failure, tubular composite

1 | INTRODUCTION

Damage in a braided composite mainly includes matrix crack, fiber breakage, and fiber-matrix debond. In other words, these are the main forms of damage in braided composite structures. As the applied stress to this structure increases, cracks grow gradually, slowly, and steadily, and the amount of damage inside the body structure increases. Eventually, the material may split into two or more pieces. Thus, the failure phenomenon occurs. Braided composite materials are usually used in high-loading capacity components. Therefore, their resistance to failure and preventing sudden failure is an important issue. Therefore, prediction of initiation and propagation of the damage is essential in the strength assessment of braided composite structures.[1–3] Understanding the stress–strain behavior and fracture characteristics is crucial in predicting the initiation and propagation of the damage in braided composite structures. By analyzing the stress levels and loadings on the structure, engineers can assess the potential for damage and implement preventative measures to avoid sudden failures. In a braided composite structure, final failure occurs suddenly. The stress–strain curve of a braided composite structure and its fracture surface is shown in Figure 1.

As can be seen in Figure 1, In the stress–strain curve of a braided composite structure as a brittle material, the material shows linear behavior until it reaches the ultimate stress point. At this point, the material fractures suddenly without any significant deformation. The fracture surface of a brittle material is usually smooth and exhibits very little plastic deformation. This is noted that Young's Law is valid in the region before the fracture. Therefore, failure prediction of a braided composite as a brittle material is a challenging task. Braid-reinforced composites exhibit different types of main failure mechanisms such as fiber/matrix interface debonding, matrix micro-cracking, and fiber breakage. However, depending on the form of the braided reinforcement used in composites, damage can include other forms of damage such as delamination.[3] Knowing about the behavior of different kinds of textile composites against various loadings (especially tensile load) and having enough information about these structures will help a lot in designing and producing breakdown-resistant products. In recent years, successful efforts have been made to model damage and its progression in textile composites, especially braided-reinforced composites under tensile loading, and some researchers showed that the braiding angle is an important parameter and affects the behavior of braided

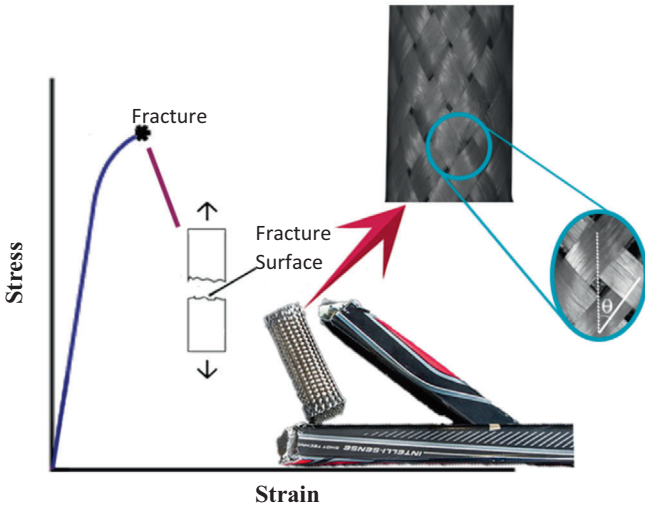

FIGURE 1 The stress–strain curve of a braided composite structure is a brittle material.

composites against the various loads.[4–7] The braiding angle is shown by Θ in Figure 1.

Li et al.[4] investigated the tensile behavior of braided composites from carbon fiber and epoxy resin at three different braiding angles (25, 35, and 45 degrees). The result showed not only the significant braiding angle role in the shear but also the damages in large strain rate load of shear. Pereira et al.[5] studied reinforced braided composite rods at braiding angles of 10°–27°. They observed that there is an optimum braiding angle of about 24° which guarantees the desired mechanical properties of their rods. The Damage of braided composites was investigated by various researchers and some of them provided methods to predict the damage progressive and failure of braided composites using numerical models.[8–17] Zhang et al.[8] studied the failure and propagation damage of a braided composite under axial tensile loading. Also, they proposed a mesoscale finite element model to predict the damage progressive in braided composites. Due to the proximity of the experimental and simulation results, it can be said that the model was accurate in simulating the damage development of this material. Singh Nobeen et al.[10] presented a numerical simulation model based on a mesoscale unit cell. Cichosz et al.[11] investigated the failure and damage of biaxial braided composites consisting of carbon fiber (HTS40) and RTM matrix under multifunctional stresses in tension and compression. The results showed an optimum braiding angle and also the forms of the composite damages. Johnston et al.[12] investigated tensile damage in triaxial braided

composites made of carbon fiber (T700S) and PR-520 resin under tensile, compressive, and shear tests in three environmental conditions, containing room temperature, hot temperature (100°C), and hot and humid (60°C and 90% humidity).? They introduced temperature and humidity as the first and second factors determining environmental conditions, respectively. Marrivada et al.[13] investigated the mechanical behavior of three-axial braided composites made of glass fibers at three braiding angles of 30°, 45°, and 60°. They observed the damages by the microscopic images and stated that the tensile properties decrease as the braid angle increases. Gautam et al.[14] investigated the effect of braiding angle and the number of axial yarns on two-dimensional flattened tubular braided composites. These composites, containing three axial yarn surfaces including 0, 6, and 12 axial yarns at three braiding angles (35, 45, and 55 degrees) were produced using carbon fiber and epoxy resin. The results showed that the failure mechanism in all samples has the same beginning and end. Mekonnen and Woo[15] studied out-of-plane and in-plane tensile and shear modulus in triaxial braided composites. They found that the presence of voids in the composite structure reduces the efficiency of the braid structure. Therefore, reduces the tensile and shear modulus. Among tensile and shear modulus, due to the presence of yarns which make the braid structure, the in-plane tensile modulus accepts the least effect. Dang et al[16] developed an analytical model in a triaxial braided composite under tensile and compressive loads and predicted the progressive damages in this structure. The basis of this model was an integrated lamination and series–parallel model that was performed through a discretization and reassembly process. The developed model using finite element was validated and the results showed that this model was credible. Zhao et al[17] investigated the failure behavior of triaxial braided composites made of T700 carbon fibers and a braiding angle of 60° under compressive. They stated that the damage in axial and transverse compression is axial yarns' micro-buckling and the accumulation of micro-cracks in the interface and matrix, respectively. Also, the results showed that the speed rate in transverse compression is more critical than in axial compression.

The VIP or VAP methods almost were used to produce a braided composite structure in all studies that are presented. Moreover, there is another method for producing a braided composite structure, which is named pultrusion or braid-trusion. These two ways are shown in Figure 2.

Ahmadi[6] used the combination of the braiding process and the pultrusion process as a new and low-cost method for producing composite rods. Both methods are known as closed mold methods and the difference between them is related to the manufactured part's specifications. The pultrusion method can be used to make any continuous piece or rod if it has a constant cross-section and no grooves or holes perpendicular to the pull direction. While the VIP method is suitable for producing large, complex, and high-quality parts, Therefore, method Pultrusion is not suitable for producing tubular composites. The VIP method will also take time and money to produce small-diameter parts.[18,19]

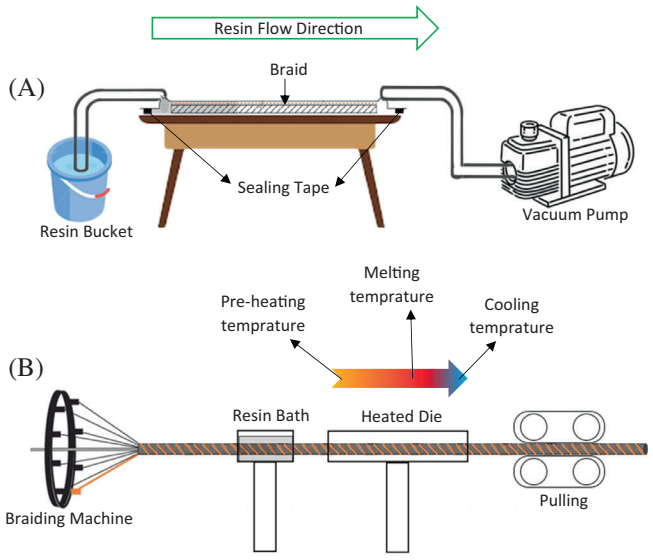

FIGURE 2 The two famous ways to braided composite production are (A) VIP method and (B) Pultrusion method.

In 2022 and 2023, efforts were made to increase the mechanical performance of different textile structures from braids as stents to woven fabrics in composites using finite element damage modeling. The results of these investigations showed that if the finite element simulation is done correctly, not only the correct prediction of the structure's performance is made, but it can also lead to proper productions and reduce the number of destructive tests and thus reduce the cost.[20–24] Also, there are some efforts to investigate the mechanical properties and fracture of braided structures and braided composites to improve the effectiveness of different braided structures and their composites.[25–27]

In this paper, a new method to produce tubular braided composites is used, which not only allows the production of tubular composite structures with small diameters but also can remove the behavior of the composite from the brittle state. It can be a starting point to enhance damage resistance and more efficiency of braided composite structures. In this study, triaxial tubular braided composite specimens are produced using two different methods. Then tensile tests are performed for prepared specimens and damage progress and events near the final failure are monitored and discussed. It is shown that the proposed manufacturing method could prevent the sudden failure of braided composites and they behave quasi-ductile manner.

2 | EXPERIMENTS

2.1 | Materials

In the current investigation, three types of yarn, namely polyester, glass, and basalt, are used to produce the specimens. The polyesters were used as braided yarns in all specimens. At the same time, the basalt and glass were used as axial yarns in separate specimens. In other words, half of the specimens are braided composites produced from polyester and glass as braids and axial yarns, and the other half from polyester and basalt as braids and axial yarns. The type of glass fiber used is E-glass. The tensile load of the used yarns which are polyester, E-glass, and basalt yarns was characterized by using an Instron 5566, according to the ASTM D 578 and the ASTM D 2256 standards.[28,29] The obtained yarns' specifications (linear density and maximum tensile load) are listed in Table 1. To determine the linear density the mass of 1000 meters of yarns which is named Tex was calculated.

TABLE 1 Properties of the yarns.

Type of yarn	Linear density (Tex)	Maximum load (N)
Polyester	256	120.67
Basalt	778	374.88
E-Glass	600	247.01

FIGURE 3 The 16-carrier vertical braiding machine.

TABLE 2 Specimens' specifications.

Braid code	Type of axial yarns	Braiding angle (degree)
B-40	Basalt	40
B-42	Basalt	42
B-44	Basalt	44
B-46	Basalt	46
G-40	Glass	40
G-42	Glass	42
G-44	Glass	44
G-46	Glass	46

The matrix materials used are R 615 and H 615 epoxy resin.

2.2 | Production process

The triaxial tubular hybrid braided specimens manufactured by a 16-carrier vertical braiding machine are shown in Figure 3. The details of specimens' codes, yarn material, and braiding angles are depicted in Table 2.

As can be seen in Table 2, each tubular triaxial hybrid braid specimen is assigned a two-part code. The first part indicates the type of axial yarn. In half of the specimens, this part is marked with the letter B and in the other half with the letter G. The letters B and G represent basalt yarn and E-Glass yarn, respectively. The second part indicates the braiding angle, with values of 40, 42, 44, and 46.

All specimens are produced at a constant braiding point to ensure consistency. In this way, none of the parameters will be insistent, and the change of braiding angle will only be due to the take-up speed changing in the braiding machine. Also, a silicone hose is used as the core during production. Therefore, the diameter of the braid and the cross-section shape of the braid remain unchanged. Then, the hybrid braid structures are cured at room temperature for 72 h by VIP, and the invented method is introduced in this study. The silicone core will be removed from the composite after the curing process. It should be noted that in the innovative method, two points should be taken into consideration before impregnating the braided structure with resin: (1) It is necessary to measure the total diameter of the braid and the inner silicon. (2) The thickness of the braid is determined and considering that this amount should make up 70% of the composite, the desired thickness for the resin is determined. Hollow silicon with a diameter equal to the

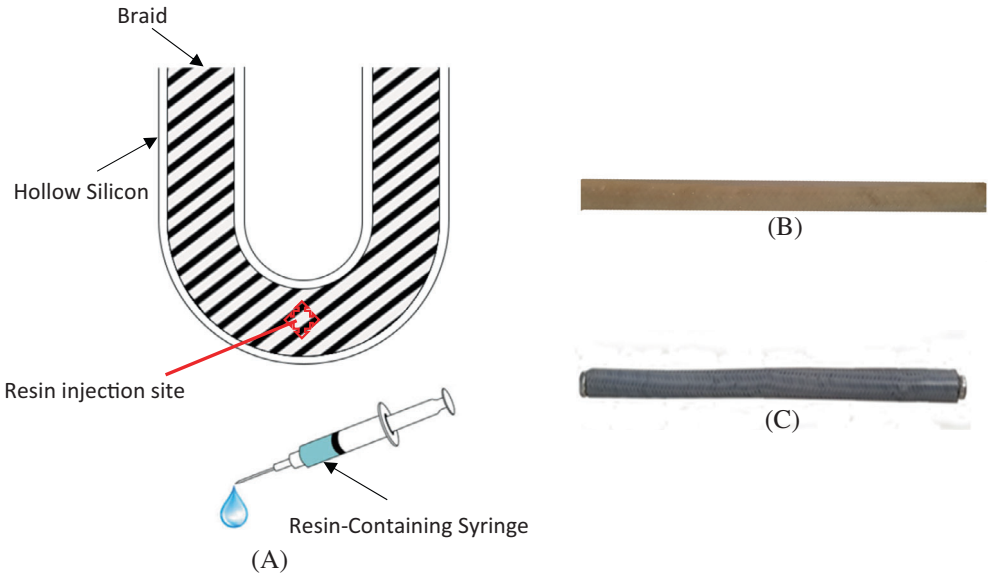

FIGURE 4 (A) The schematic of the invented method. (B) The braided composite specimen produced by the VIP method. (C) The braided composite specimen produced by the invented method.

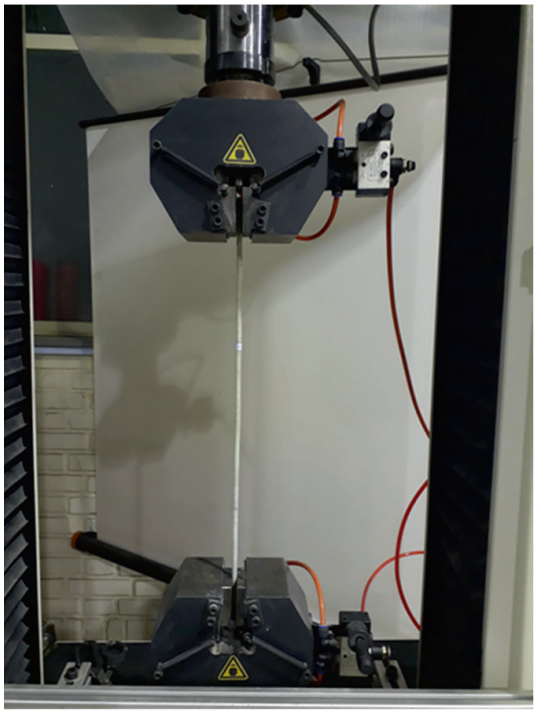

FIGURE 5 SANTAM tensile testing machine.

calculated diameter for the composite is prepared, and the braid is placed inside it to inject the resin according to the schematic shown in Figure 4A. After curing the resin, the composite is easily removed from the silicon. The thickness of these composite tubes is almost 1.5 mm. The tubular braided composite specimens which are produced by VIP and invented method are shown in Figure 4B,C, respectively. As can be seen, the specimen produced by the invented method has a uniform, smooth, and polished surface.

2.3 | Tensile test

The tensile tests of specimens are carried out, in two specimen lengths of 12 and 30 cm for each one using a SANTAM tensile machine with a capacity of 15 tons shown in Figure 5.

Since the similar form of hybrid braided composites produced in this research was not widely observed in other research works and common standards, to determine the length of the samples under the uniaxial tensile test, the sources that were most similar to the present work (the tubular samples, etc.) were noticed. After the two selected lengths showed almost the same results in a series, due to less consumption of raw materials, the shorter length was chosen to perform the uniaxial tensile test on the other samples.

The tensile tests are performed at a temperature of 25 ± 2 ° C and a relative humidity of 65 ± 5%. The constant loading speed is 3 mm/min, and the test gauge length is approximately 67% of the specimen's length. Each specimen is tested in five replications, and the mean tensile load in 5 measurements is considered the final value for that specimen. A total of 85 specimens are tested.

3 | DAMAGE AND TENSILE FAILURE ANALYSIS

3.1 | Experimental analysis

To investigate the composite's damage, microscopic images before and after the tensile test were taken from the surface of the braided reinforced composites, as shown in Figures 6 and 7.

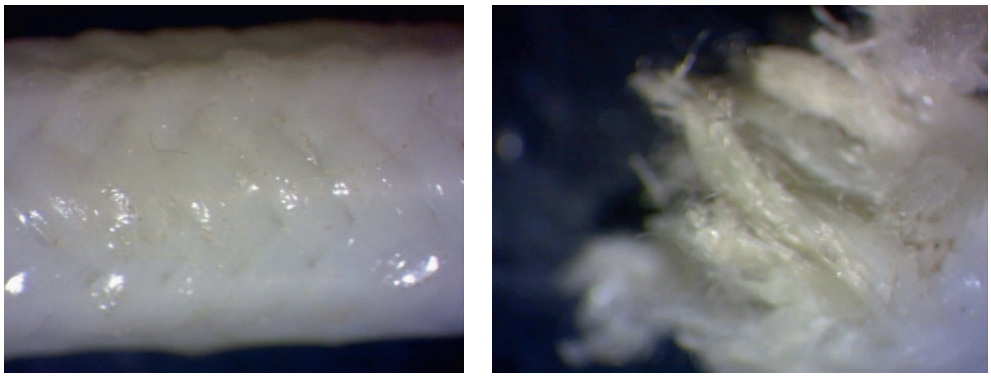

(A) (B)

FIGURE 6 The surface of the braided reinforced composites produced by the VIP method (A) before the tensile test and (B) after the tensile test.

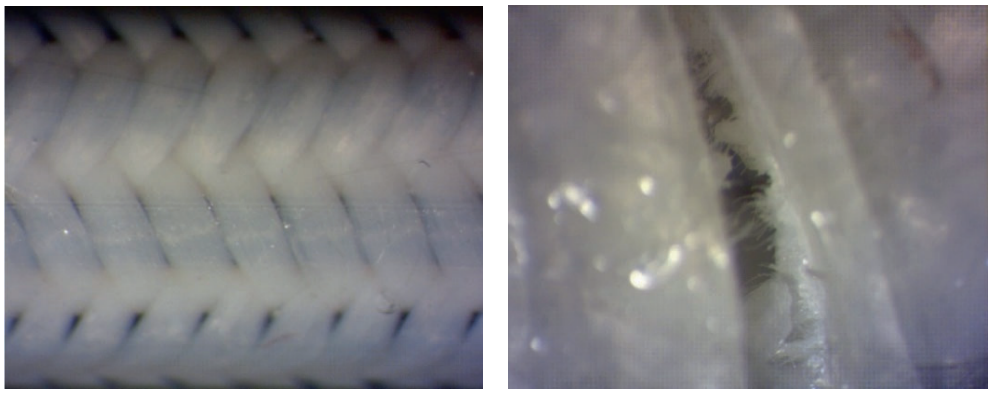

(A) (B)

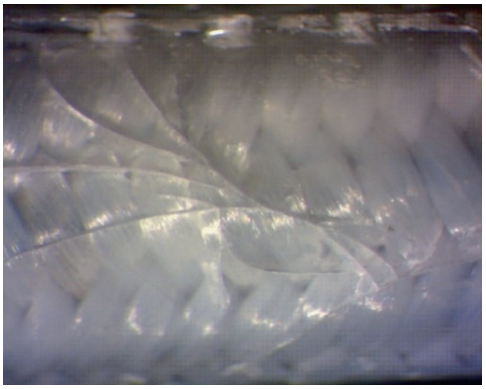

(C)

FIGURE 7 The surface of the braided reinforced composites produced by the invented method (A) before the tensile test, (B) after the tensile test on reinforcement, and (C) after the tensile test on matrix.

As can be seen, In the composite braid produced by the VIP method, the structure is practically splitting into two pieces, with no cracks on the matrix. Therefore, the braided reinforced composite produced in terms of strength is almost the same at all points. The damage of the composite, caused by tension, rapidly grows, and causes failure. In this method, a thin surface of the resin is placed on the braid structure. Therefore, as soon as the damage occurs when tension is applied to the composite structure, it rapidly grows and causes structural damage. After the tensile test, the only visible damage to the composite is the breakage of the three-axial hybrid braid structure and the fragmentation of the hybrid-reinforced composite. In contrast, the method used by the researchers in this study resulted in a braided composite structure with a uniform surface. As a result, structural reinforcement has occurred in parts of the braid that are curved inwards compared to conventional resin methods. This provided structural reinforcement in previously vulnerable areas, enabling the composite structure to withstand more force. In addition, damage starts in weaker parts and progresses step

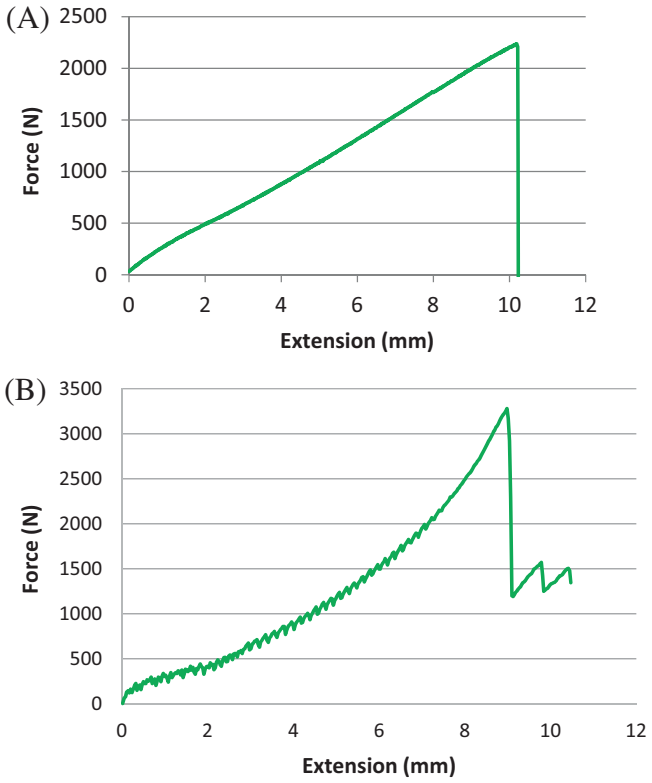

FIGURE 8 Force-Extension diagram of the braided reinforced composites (A) produced by the VIP method and (B) produced by the invented method.

by step, including matrix cracking in parts of the damaged structure. In other words, the braided composites produced by the invented method not only can endure against high tensile loads but also still maintain their efficiency even in the presence of cracks.

A Force-Extension diagram of a tensile test for hybrid-reinforced composites produced by VIP and invent method is shown in Figure 8A,B, respectively. According to this figure, the damage and failure of the composite structure production by the VIP method is a brittle fracture, where the damage rapidly grows in the matrix and braid structure, leading to immediate failure. In contrast, the composite structure produced using the invented method experienced failure in several stages. The climax of the graph is the point where the damage at one of these points rapidly grows and proceeds almost to the final failure, and a sharp drop in force occurs suddenly. However, the structure does not split into two parts and the damage progresses to differen0t parts of the structure. This was evident from the visible injuries in the matrix and braid structure of the composite. Therefore, we can say that the use of the invented resin method causes this structure not to suddenly fail after reaching the maximum tensile force. In fact, after the peak, the failure of the composite will continue in some stages.

Furthermore, using the invented resin method resulted in slight changes in the tensile properties of the composite. The force and extension increased, while the modulus decreased. This suggests that the invented method can enhance the overall performance of the braided composite structure. It is noticed that in general, the samples produced by the same method have the same general diagram shape. In other words, all of the samples produced by the VIP method have the same diagram shape, and all of the samples produced by the invented method have the same diagram shape. Even the length specimen does not affect the diagram shape and specimens produced by the same method in different specimen lengths not only had no difference but also had very close results. Also, repetition tests of each sample had results very close to the average value.

3.2 | Theoretical analysis

The braided composites studied in this research consist of the triaxial hybrid braid and the resin. Therefore, mixing rules can be used to predict the tensile modulus. So, it is first necessary to predict the tensile modulus of the braid and its volume fraction. To predict the tensile modulus of triaxial hybrid braided structures Equation (1), presented by Boris, has used[30]:

$$E_{\text{braid}} = N_{\text{bias}} E_{\alpha} \cos^4(\alpha) + N_{\text{axial}} E_{\alpha} \quad (1)$$

where E_{Braid}, E_{α}, α, N_{bias}, and N_{axial} are the modulus of the braid, the Modulus for a yarn, the braiding angle, the number of biases, and axial yarns, respectively.

Equation (1) is modified with the following points and assumptions:

1. The bias yarns and the axial yarns are different.
2. The bias yarns have the tensile modulus E_{bias} and the yarn count in Tex T_{bias}.
3. The axial yarns have the tensile modulus E_{axial} and the yarn count in Tex T_{axial}.
4. A hybrid braided structure can be known as a composite structure. Therefore, all the rules governing composite also apply to hybrid braided structures.
5. The unit of the modulus is in centinewton per tex.

Therefore, Equation (1) for a two-component system will be written as follows:

$$E_{\text{braid}} = N_{\text{bias}} E_{\text{bias}} \cos^4(\alpha) + N_{\text{axial}} E_{\text{axial}} \quad (2)$$

Then, according to the Classical Lamination Theory, a coefficient of the yarn count is used in the braid structure, and Equation (3) is introduced as the equation to

predict the tensile modulus of triaxial hybrid braids with axial yarn.

$$E_{\text{braid}} = \frac{\text{Tex}_{\text{bias}}}{\text{Tex}_{\text{braid}}} N_{\text{bias}} E_{\text{bias}} \cos^4(\alpha) + \frac{\text{Tex}_{\text{axial}}}{\text{Tex}_{\text{braid}}} N_{\text{axial}} E_{\text{axial}} \tag{3}$$

where $\text{Tex}_{\text{braid}}$ is the count of triaxial hybrid braided structure. Also, E_{braid} is the tensile modulus of the reinforcing phase in the composite.

The volume fraction of reinforcing fibers ($V_{\text{reinforcement}}$) in a composite structure is one of the most influential factors in predicting its strength and mechanical properties. The tubular braided reinforcement structure is not only the void but also the hollow structure. One of the practical and general equations for calculating the volume fraction of fibers in the braid structure, Equation (4), has been used to predict[31]:

$$V_{\text{reinforcement}} = V_{\text{f}} = \frac{N.(1+c).T}{10^6.\pi.\rho.t.D.cos\theta} \tag{4}$$

where N is the number of yarn carriers, c is the crimp ratio due to yarn interlacement, T is the linear density (Tex) of the yarn in g/km, ρ is the density of the yarn used in the braid structure, D is the effective braid diameter, t is the thickness, and θ is the braiding angle.

The above equation, rewritten with the consideration of various assumptions had led to the presented Equation (5):

1. The amount of crimp ratio for axial yarns is equal to zero.
2. The confinement of the axial yarns by the bias yarns causes their thickness to be limited.
3. The braiding angle of the axial yarns is equal to zero

$$V_{\text{f}} = \frac{N_{\text{bias}}.(1+c).T_{\text{bias}}}{10^6.\pi.\rho_{\text{bias}}.t_{\text{bias}}.D_{\text{bias}}.\cos\theta} + \frac{N_{\text{axial}}.T_{\text{axial}}}{10^6.\pi.\rho_{\text{axial}}.t_{\text{axial}}.D_{\text{axial}}} \tag{5}$$

In the above equation, indices axial and bias refer to the axial yarns and bias yarns used in the hybrid braided structure, respectively.

Finally, the predictions made in Equation (6) were replaced. It should be noted that according to the calculations made in the innovative method, the volume fraction of the resin is equal to 0.3 in the whole composite.

$$E_{\text{composite}} = V_{\text{reinforcement}} E_{\text{reinforcement}} + V_{\text{resin}} E_{\text{resin}} \tag{6}$$

3.3 | Damage simulation by FEM

In this paper, for modeling the effects of damages in reinforced composite with triaxial hybrid braid used the three-dimensional Hashin damage criterion.

The tubular composites produced in this study have a small diameter. Therefore, a tubular braided composite can be considered in the form of a composite shell. As shown in Figure 9, the braided structure in this shell is a two-layer of single-sided fibers with angles $+\theta$ and $-\theta$. Also, axial yarns were placed as a layer of single-sided fibers with an angle of zero between those two layers. Because the Hashin criterion applies to a unidirectional single-sided, a reinforced composite with a triaxial hybrid braid is modeled as a multilayer composite cylinder. It can be said that each layer is considered a unidirectional composite layer. Due to the symmetry of this structure, its geometry can be defined as an eighth sector considered.

Then, engineering constants and other required parameters to use the Hashin criteria are calculated using micromechanical rules and available information on the estimated properties of fibers and resins. Equations (7)–(10) are used to calculate the strength values used for this criterion in 3D[2]:

$$F_{\text{ft}} = \left(\frac{\sigma_{11}}{X_{\text{T}}}\right)^2 + \frac{1}{S_{\text{l}}}\left(\sigma_{12}{}^2 + \sigma_{13}{}^2\right) \le 1 \qquad \sigma_{11} \ge 0 \tag{7}$$

$$F_{\text{fc}} = \frac{\sigma_{11}}{-X_{\text{C}}} \le 1 \qquad \sigma_{11} < 0 \tag{8}$$

$$F_{\text{mt}} = \frac{1}{Y_T{}^2}(\sigma_{22}+\sigma_{33})^2 + \frac{1}{S_T{}^2}\left(\sigma_{23}{}^2 + \sigma_{22}\sigma_{33}\right) + \frac{1}{S_l{}^2}\left(\sigma_{12}{}^2 + \sigma_{13}{}^2\right) \le 1 \qquad \sigma_{22}+\sigma_{33} \ge 0 \tag{9}$$

$$F_{\text{mc}} = \frac{1}{Y_C}\left[\left(\frac{\sigma_{22}}{2S_T}\right)^2 - 1\right](\sigma_{22}+\sigma_{33}) + \frac{1}{4S_T{}^2}(\sigma_{22}+\sigma_{33})^2 + \frac{1}{S_T{}^2}\left(\sigma_{23}{}^2 - \sigma_{22}\sigma_{33}\right) + \frac{1}{S_l{}^2}\left(\sigma_{12}{}^2 + \sigma_{13}{}^2\right) \le 1 \qquad \sigma_{22}+\sigma_{33} < 0 \tag{10}$$

where σ_{11}, σ_{22}, and σ_{33} are the normal stress components in the direction of the fibers, perpendicular to the fibers and perpendicular to the fibers out of the plane, respectively. σ_{12}, σ_{23}, and σ_{13} are also shear stresses. These parameters are expressed as the mechanical properties of an orthotropic single-layer composite according to the stress–strain relationship in the form of Equation (11)[32]:

$$\begin{Bmatrix}\sigma_{11}\\ \sigma_{22}\\ \sigma_{33}\\ \sigma_{12}\\ \sigma_{13}\\ \sigma_{23}\end{Bmatrix}=\begin{bmatrix}C_{11} & C_{12} & C_{13} & 0 & 0 & 0\\ C_{12} & C_{22} & C_{23} & 0 & 0 & 0\\ C_{13} & C_{23} & C_{33} & 0 & 0 & 0\\ 0 & 0 & 0 & G_{12} & 0 & 0\\ 0 & 0 & 0 & 0 & G_{13} & 0\\ 0 & 0 & 0 & 0 & 0 & G_{23}\end{bmatrix}\begin{Bmatrix}\varepsilon_{11}\\ \varepsilon_{22}\\ \varepsilon_{33}\\ \varepsilon_{12}\\ \varepsilon_{13}\\ \varepsilon_{23}\end{Bmatrix} \quad (11)$$

After the onset of damage, the stiffness matrix is affected by the damage parameters, and with their increase, the initial value of the stiffness decreases. Therefore, the stress component values are constantly updated in finite element analysis.

The other parameters used in Equations (7)–(10), that is, XT, XC, YT, YC, ST, and Sl, which are fiber tensile strength, fiber compressive strength, matrix tensile strength, matrix compressive strength, longitudinal shear strength, and transverse shear strength, respectively, and are required as inputs to the finite element analysis. Therefore, these parameters are measured by different experimental and mathematical methods and are listed in Table 3.

As mentioned, due to the symmetry of the structure, instead of modeling the entire tubular composite, only one-eighth of it is modeled. Therefore, the boundary conditions, meshing, and the results obtained for this model are presented in the following.

As can be seen in Figure 10, in the side 1, the degrees of freedom are closed in the direction of force (Z) and open in both radial and circumferential directions (r and θ) and it is possible to move. In the side 2, which is also the direction of loading, it is possible to move only in the direction of the force and perpendicular to it in the circumferential direction, and it is not possible to move in the direction perpendicular to the fibers in the radial direction. On the sides of the one-eighth sector, that is, side 3 and side 4, the degrees of freedom are closed in the circumferential direction (θ) and it is possible to move in the directions of force (z) and radial (r). In the side 1 and in a node that has a common border with one of the sides, that is, side 3 or side 4, to prevent the movement of the rigid body in all degrees of freedom in the direction of force (z), radial (r), and environment (θ) is closed. In other words, in this part, the

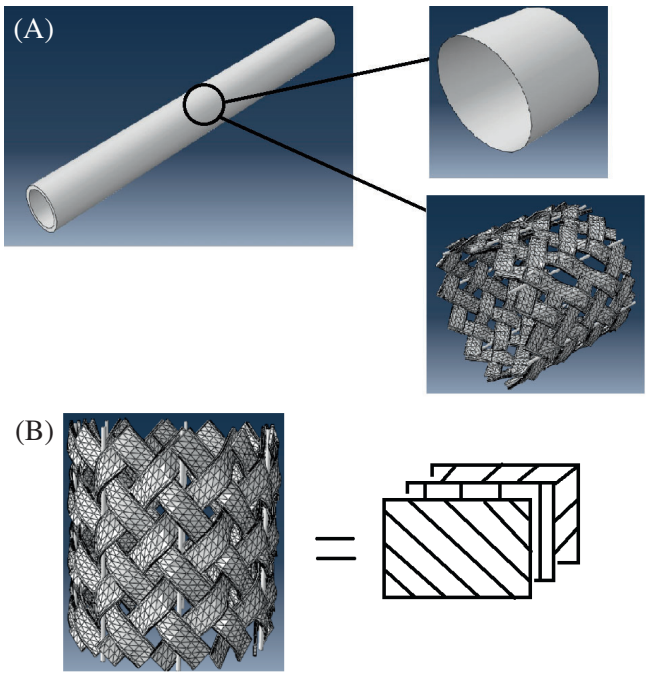

FIGURE 9 Simplified structure (A) the composite specimen and (B) a triaxial braid.

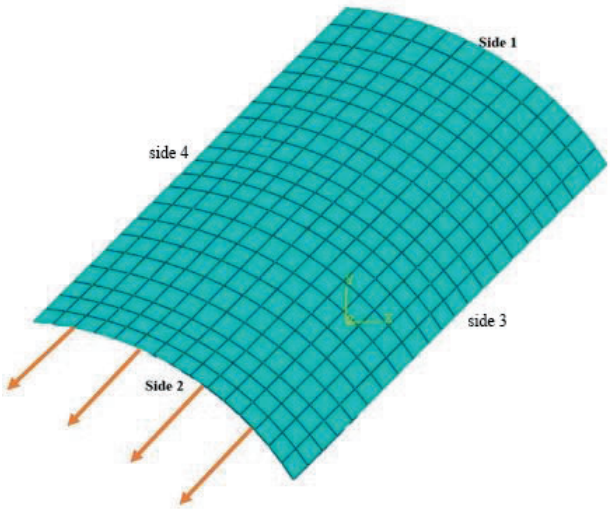

FIGURE 10 Meshing, loading, and boundary conditions in the RVE.

TABLE 3 Required parameter values for the Hashin criterion.

Parameter	X_T (MPa)	X_C (MPa)	Y_T (MPa)	Y_C (MPa)	S_T (MPa)	S_l (MPa)	Breaking energy			
							Fiber tensile (N/mm)	Fiber compressive (N/mm)	Matrix tensile (N/mm)	Matrix compressive (N/mm)
Value	600	300	20	75	43	43	50	55	0.15	0.15

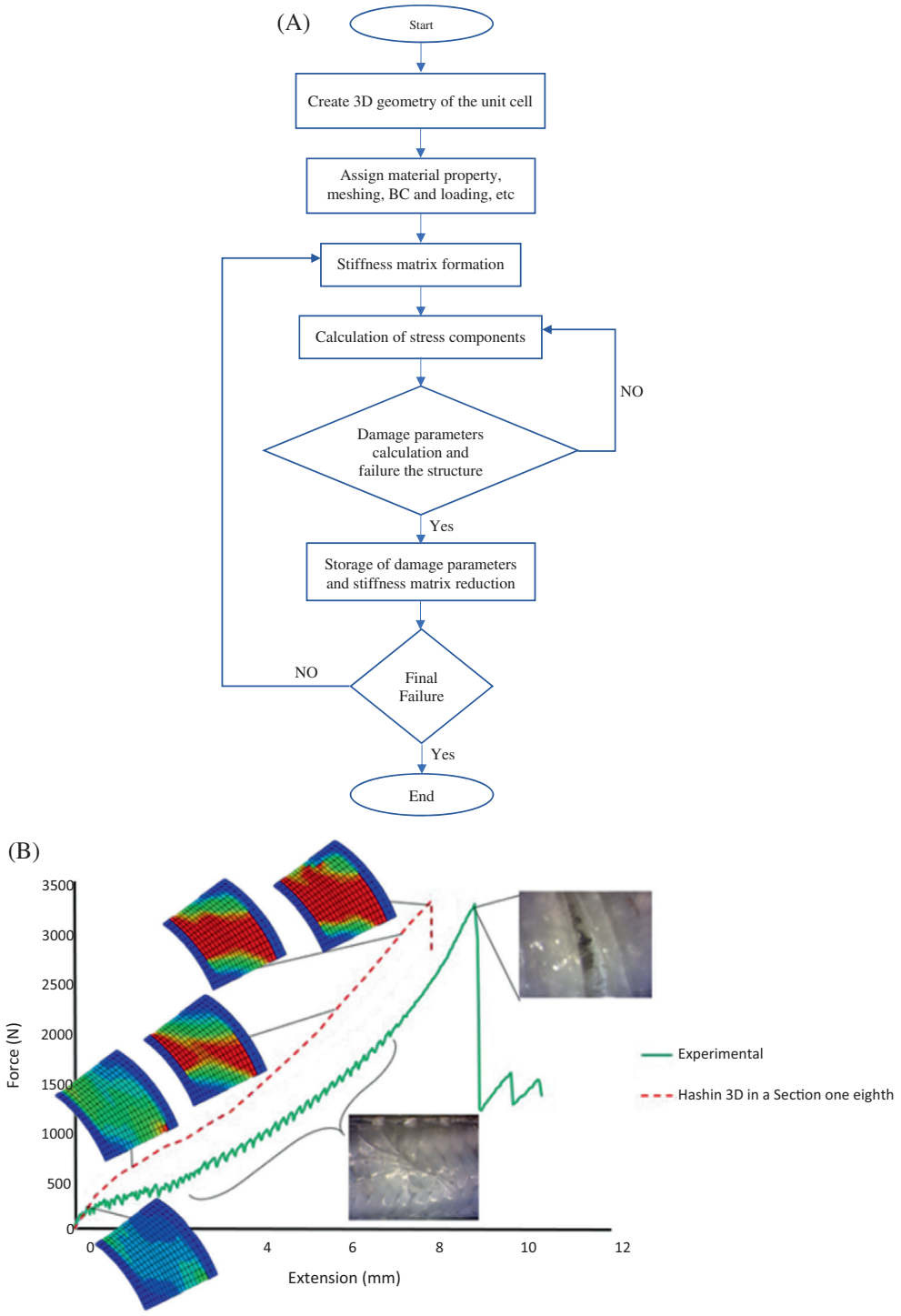

FIGURE 11 (A) Damage processing of FEM method flowchart. (B) Tensile force/elongation curve of triaxial tubular braided composites with a braiding angle of 40° and glass axial yarns related to experiments and FEM analysis.

boundary conditions of the support are taken into account and the possibility of all linear and rotational displacements is zero. Also, SC8R is used for the mesh design. The flowchart of the FEM analysis process algorithm is shown in Figure 11A. The tensile force/extension curve in Figure 11B not only compared the predicted results which are obtained by FEM analysis with the experiment results but also demonstrated the failure statuses related to experimental and FEM analysis.

As can be seen in Figure 11B, the behavior of the obtained results by FEM analysis is in good agreement with the experimental results. It indicates that the process of simulating, and selecting the damage criterion, and how to define it are appropriate. In addition, the amounts of fracture load and displacement predicted by the numerical solution are more and smaller than the experimental values, respectively. It should be noted that not considering some defects, such as geometric and

structural defects, and not considering the inter-layer separation phenomenon causes the structure stiffness in numerical modeling to become more than the real value. Therefore, the force that the structure can withstand in a certain displacement will have more in the numerical results than in the experimental results. On the other hand, a graph that has a greater slope will reach this value faster. Therefore, it will have less movement in this situation. Also, the failure status at the numerical solution (FEM) curve showed that despite the damage progressive, the structure still retains its efficiency. Because the red color, which indicates the presence of the greatest stress in the structure, is observed only in a small point of the representative element, not in the structure's representative element entirety. Therefore, not only will the damage grow gradually, but the final failure will also come out of the brittle state and will not occur suddenly. This can also be seen in the experimental curve. There are four different types of damage or failure in composite structures at tensile and compressive including transverse cracking of the matrix, fiber breakage, shear of fibers and matrix, and delamination. To determine the type of damage in this research, the results of finite element analysis of the triaxial hybrid braided reinforced composite for each layer were investigated separately. Detailed investigations showed that the damage starts as a fracture of the axial fibers inside the tubular composite, then the damage in the direction of the thickness toward the outer surface of the tubular composite and the formation of a matrix crack on the outer surface of the tubular composite is visible. The damage continues in the form of delamination or separation, and the curve reaches its peak with the failure of the braid. Therefore, the effective damage mechanisms in this research include fiber breakage, matrix cracking, and delamination in order of priority.

4 | RESULTS AND DISCUSSION

4.1 | Effect of resin method on tensile properties

The Experimental tensile test values on hybrid-reinforced composites, produced by two different methods, are tabulated in Table 4.

Each composite is assigned a four-part code. The first part indicates the composite production method that is marked with V and I for the VIP and invented method, respectively. The second part is marked with E because they are experimental results. The third and fourth parts are similar to coding in Table 2.

As can be seen, the use of the invented resin method reduces the tensile modulus. Using this method, the excess amount of resin that creates a uniform surface on

TABLE 4 The tensile modulus of the samples.

Composite code	V-E-B-40	V-E-B-42	V-E-B-44	V-E-B-46	Comments
Tensile modulus (cN/Tex)	7.73	7.50	7.28	7.02	Braided composites specimens which are produced by VIP method
Composite code	V-E-G-40	V-E-G-42	V-E-G-44	V-E-G-46	
Tensile modulus (cN/Tex)	5.29	5.00	4.89	4.65	
Composite code	I-E-B-40	I-E-B-42	I-E-B-44	I-E-B-46	Comments
Tensile modulus (cN/Tex)	5.76	5.52	5.51	5.44	Braided composite specimens which are produced by invented method
Composite code	I-E-G-40	I-E-G-42	I-E-G-44	I-E-G-46	
Tensile modulus (cN/Tex)	3.27	3.14	3.12	3.09	

TABLE 5 The prediction tensile modulus of the samples.

Composite code	V-T-B-40	V-T-B-42	V-T-B-44	V-T-B-46	Comments
Tensile modulus (cN/Tex)	7.91	7.84	7.78	7.73	Braided composite specimens which are produced by VIP method
Composite code	V-T-G-40	V-T-G-42	V-T-G-44	V-T-G-46	
Tensile modulus (cN/Tex)	6.06	5.97	5.90	5.83	
Composite code	I-T-B-40	I-T-B-42	I-T-B-44	I-T-B-46	Comments
Tensile modulus (cN/Tex)	7.28	7.21	7.15	7.10	Braided composite specimens which are produced by invented method
Composite code	I-T-G-40	I-T-G-42	I-T-G-44	I-T-G-46	
Tensile modulus (cN/Tex)	5.38	5.30	5.22	5.16	

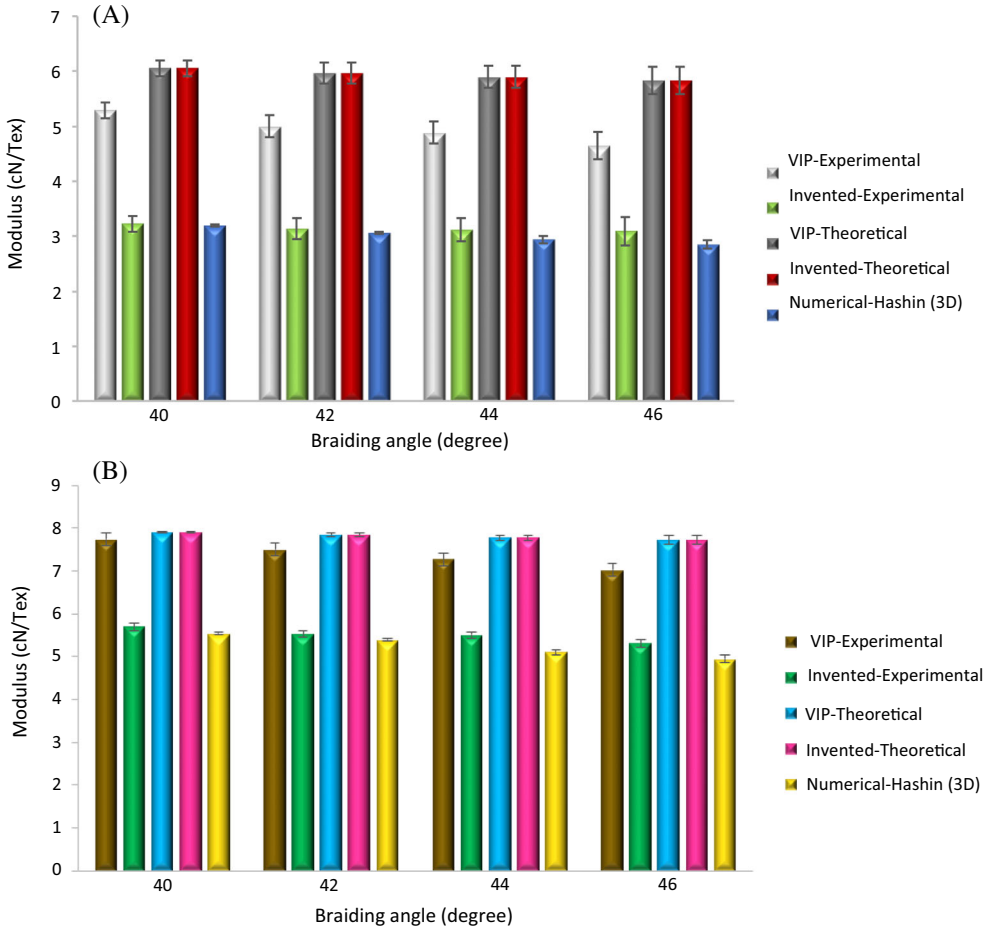

FIGURE 12 Comparison of tensile modulus results in triaxial hybrid braided composites (A) with glass-axial yarn and (B) with basalt-axial yarn.

the braided composite increases the mass and strength of the composite. The tensile strength of the composite is dependent on the action of the braid and the resin. So, the amount of increase in force is less than the mass. Therefore, the modulus decreases.

4.2 | Theoretical model and FEM analysis

The theoretical results are tabulated in Table 5. Also, the results of the theoretical and numerical predictions were compared with the experimental results in Figure 12A,B.

Each composite is assigned a four-part code. The first part indicates the composite production method that is marked with *V* and *I* for the VIP and invented method, respectively. The second part is marked with *T* because they are Theoretical results. The third and fourth parts are similar to coding in Table 2.

As can be seen, the predicted values are higher than the experimental values. Also, the values theoretical predicted in the VIP Method are closer than the invented method to the experimental values. The values obtained from the FEM or numerical method are very close to the invented method in experiments. Therefore, this numerical method provided a good prediction from the new method of resin injection and tubular hybrid braided composite production.

5 | CONCLUSIONS

In the current work, the role of the composite production method on tensile behavior was investigated. The eight different triaxial hybrid braided composite structures made of two yarn types were produced and evaluated in this study. Figured out that the production method of a composite structure plays an essential role in damage behavior, affects the tensile modulus, and has a significant impact on its tensile behavior. However, a decrease in the tensile modulus of the triaxial tubular braided composite produced by the invented method is not very noticeable. There are several curved parts inwards on the braided composite structure, and a concentration of tension occurs at these points. The innovative technique used in this paper reinforces these points. Therefore, the hybrid braided composite structure can withstand more load and time until the moment of final failure. Also, the

damage does not cause a sudden failure but continues step by step. It seems that using this method can be a step towards creating quasi-ductile behavior in hybrid tubular braided reinforced composites.

Also, in this study, some equations were developed to predict the volume fraction of the reinforcement phase in a triaxial hybrid braided composite structure and its tensile modulus. These equations provided a relatively good approximation. Therefore, it seems that they can perform well in forecasting.

The finite element simulation performed for damage occurred in tubular triaxial hybrid braided composite structures considering this structure in the form of a shell. The results confirm that the damage is gradual and not suddenly progressive. The effective Damage mechanisms in the tubular hybrid braided composite samples examined in this research include fiber breakage, matrix cracking, and delamination in order of priority. These damage mechanisms agree with previous works investigated by the others.

DATA AVAILABILITY STATEMENT

All data have been reported in this paper.

ORCID

Mahdi Bodaghi https://orcid.org/0000-0002-0707-944X

REFERENCES

1. Anderson TL. *Fracture Mechanics: Fundamentals and Applications*. Third ed. Taylor & Francis; 2005.
2. Zhong Y, Suraj R, Wang C, Chia ESM, Joshi SC, Chen Z. Damage advancement behavior in braided composite structures for mini aerial vehicles. *Mech Adv Mater Struct*. 2018;25(11):889-900. doi:10.1080/15376494.2017.1310335
3. Fouinneteau M. Damage and Failure Modelling of Carbon and Glass 2D Braided Composites, PhD thesis, Cranfield University. 2006 http://hdl.handle.net/1826/1555
4. Li Y, Gan X, Gu B, Sun B. Dynamic responses and damage evolutions of four-step three-dimensional braided composites subjected to high strain rate punch shear loading. *J Compos Mater*. 2015;50(12):1635-1650. doi:10.1177/0021998315595114
5. Pereira CG, Fangueiro R, Jalali S, Araujo M, Marque P. Braided reinforcement composite rods for the internal reinforcement of concrete. *Mech Compos Mater*. 2008;44(3):221-230. doi:10.1007/s11029-008-9015-z
6. Ahmadi MS, Johari MS, Sadighi M, Esfandeh M. An experimental study on mechanical properties of GFRP braid-pultruded composite rods. *Express Polym Lett*. 2009;9(3):560-568. doi:10.3144/expresspolymlett.2009.70
7. Cao H, Chen H. Influence of braided angles on mechanical properties of three-dimentional full five direction braided composites. *J Text Eng Fash Technol*. 2017;1(3):1-6.
8. Zhang C, Li N, Wang W, Binienda WK, Fang H. Progressive damage simulation of triaxially braided composite using a 3D meso-scale finite element model. *Compos Struct*. 2015;125:104-116. doi:10.1016/j.compstruct.2015.01.034
9. Dai S, Cunningham PR. Multi-scale damage modelling of 3D woven composites under uni-axial tension. *Compos Struct*. 2016;142:298-312. doi:10.1016/j.compstruct.2016.01.103
10. Nobeen NS, Zhong Y, Francis BAP, et al. Constituent materials micro-damage modeling in predicting progressive failure of braided fiber composites. *Compos Struct*. 2016;145:194-202. doi:10.1016/j.compstruct.2016.02.078
11. Cichosz J, Wehrkamp-Richter T, Koerber H, Hinterhölzl R, Camanho PP. Failure and damage characterization of (±30o) biaxial braided composites under multiaxial stress states, compos. Part a. *Appl Sci*. 2016;90:748-759. doi:10.1016/j.compositesa.2016.08.002
12. Johnston JP, Liu KC, Yekani Fard M, Chattopadhyay A. Mechanical properties and damage characterization of triaxial braided composites in environmental conditions. *J Compos Mater*. 2017;51(1):67-80. doi:10.1177/0021998316636456
13. Marrivada GV, Chaganti PK, Sujith R. Fabrication and mechanical characterization of glass fibre reinforced triaxially braided composites. *J Compos Mater*. 2020;55(3):361-376. doi:10.1177/0021998320948932
14. Gautam M, Sivakumar S, Barnett A, Barbour S, Ogin SL, Potluri P. On the behaviour of flattened tubular Bi-axial and tri-axial braided composites in tension. *Compos Struct*. 2021;261:113325. doi:10.1016/j.compstruct.2020.113325
15. Mekonnen AA, Woo K. Effects of defects on effective material properties of triaxial braided textile composite. *Int J Aeronaut Space Sci*. 2020;21(3):657-669. doi:10.1007/s42405-019-00244-8
16. Dang H, Zhao Z, Liu P, Zhang C, Tong L, Li Y. A new analytical method for progressive failure analysis of two-dimensional triaxially braided composites. *Compos Sci Technol*. 2020;186:107936. doi:10.1016/j.compscitech.2019.107936
17. Zhao Z, Liu P, Dang H, et al. Effects of loading rate and loading direction on the compressive failure behavior of a 2D triaxially braided composite. *Int J Impact Eng*. 2021;156:103928. doi:10.1016/j.ijimpeng.2021.103928
18. https://composites.ugent.be/home_made_composites/documentation/FibreGlast_Vacuum_infusion_process.pdf
19. Minchenkov K, Vedernikov A, Safonov A, Akhatov I. Thermoplastic pultrusion: a review. *Polymer*. 2021;13(2):180. doi:10.3390/polym13020180
20. Jiang H, Ziegler H, Zhang Z, et al. 3D printed tubular lattice metamaterials for mechanically robust stents. *Compos B: Eng*. 2022;236:109809. doi:10.1016/j.compositesb.2022.109809
21. Zhang X, Xiao Y, Meyer CS, O'Brien DJ, Ghosh S. Impact damage modeling in woven composites with two-level parametrically-Upscaled continuum damage mechanics models (PUCDM). *Compos B: Eng*. 2022;233:109607. doi:10.1016/j.compositesb.2021.109607
22. Li X, Luo Y, Yang F, et al. In situ-formed micro silk fibroin composite sutures for pain management and anti-infection. *Compos B: Eng*. 2023;260:110729. doi:10.1016/j.compositesb.2023.110729
23. Volk M, Yuksel O, Baran I, Hattel JH, Spangenberg J, Sandberg M. Cost-efficient, automated, and sustainable composite profile manufacture: a review of the state of the art, innovations, and future of pultrusion technologies. *Compos B: Eng*. 2022;246:110135. doi:10.1016/j.compositesb.2022.110135

24. Wang Z, Luo J, Gong Z, Luo Q, Li Q, Sun G. On correlation of stamping process with fiber angle variation and structural performance of thermoplastic composites. *Compos B: Eng*. 2022; 247:110270. doi:10.1016/j.compositesb.2022.110270
25. Ghamkhar G, Johari MS, Toudeshky HH, Bodaghi M. An experimentally validated model for predicting the tensile modulus of tubular biaxial and triaxial hybrid braids. *Polym Compos*. 2022;43(12):9000-9011. doi:10.1002/pc.27079
26. Mojarrad MZ, Dabiryan H, Gharehaghaji AA, Rezadoust AM. Analyzing the effect of fiber path curvature on the fracture behavior of braided composite cylinders; experimental study. *Polym Compos*. 2023;45:1378-1390. doi:10.1002/pc.27860
27. Luo H, Wang Q, Yang Y, et al. Experimental study on the mechanical properties of three-dimensional braided composite circular tubes with preembedded licker-in. *Polym Compos*. 2023;44(9):5433-5449. doi:10.1002/pc.27499
28. Standard Specification for Glass Fiber Strands. *ASTM International: West Conshohocken*. PA; 2018.
29. Standard Test Method for Tensile Properties of Yarns by the Single-Strand Method. ASTM International.
30. Boris D, Xavier L, Damien S. The tensile behaviour of biaxial and triaxial braided fabrics. *J Ind Text*. 2018;47(8):2184-2204. doi:10.1177/1528083716654469
31. Potluri P, Rawal A, Rivaldi M, Porat I. Geometrical modelling and control of a triaxial braiding machine for producing 3D preforms. *Compos Part A: Appl Sci Manuf*. 2003;34(6):481-492. doi:10.1016/S1359-835X(03)00061-7
32. Pederson J. Finite element analysis of carbon fiber composite ripping using abaqus, Clemson University, USA. 2008.

How to cite this article: Ghamkhar G, Johari MS, Bodaghi M. Enhancing damage resistance in tubular triaxial hybrid braided composites: Innovative production and tensile modulus prediction with damage analysis. *Polym Compos*. 2024;1-14. doi:10.1002/pc.28328